Syntheses, Crystal Structures and Electronic Properties of $[Cu(bipym)(C_4O_4)(H_2O)_3]\cdot 2H_2O$ and $[Cu_2(bipym)(C_4O_4)_2(H_2O)_6]$ (bipym = 2,2′-bipyrimidine)†

Isabel Castro,[a] Jorunn Sletten,[b] Lisbeth K. Glærum,[b] Juan Cano,[a] Francesc Lloret,[a] Juan Faus[a] and Miguel Julve*[,a]

[a] *Departament de Química Inorgànica, Facultat de Química de la Universitat de València, Dr. Moliner 50, 46100 Burjassot (València), Spain*

[b] *Kjemisk Institutt, Universitetet i Bergen, 5007 Bergen, Norway*

Two new mixed-ligand complexes $[Cu(bipym)(C_4O_4)(H_2O)_3]\cdot 2H_2O$ **1** and $[Cu_2(bipym)(C_4O_4)_2(H_2O)_6]$ **2** [bipym = 2,2′-bipyrimidine and $C_4O_4^{2-}$ = dianion of squaric acid (3,4-dihydroxycyclobut-3-ene-1,2-dione)] have been obtained from aqueous solutions containing $Cu(NO_3)_2\cdot 3H_2O$, bipym and $Li_2[C_4O_4]$ in 1:1:0.25 and 2:1:0.5 (Cu^{2+}:bipym:$C_4O_4^{2-}$) molar ratio, respectively. The structures of both complexes have been characterized by single-crystal X-ray analysis. Compound **1** consists of mononuclear $[Cu(bipym)(C_4O_4)(H_2O)_3]$ units in which the copper atom exhibits a slightly distorted elongated-octahedral co-ordination with two bipym nitrogens, one squarate oxygen and one water oxygen forming the equatorial plane, and two water molecules in the axial positions. The structure of **2** is built by centrosymmetric bipym-bridged dinuclear $[Cu_2(bipym)(C_4O_4)_2(H_2O)_6]$ units, the geometry of each copper atom being similar to that found in **1**. Squarate acts as a monodentate ligand in both compounds whereas bipym exhibits chelating and bis(chelating) co-ordination modes in **1** and **2**, respectively. The intramolecular metal–metal separation in **2** [5.542(1) Å] is the largest found in bipym-bridged copper(II) complexes. The magnetic behaviour of **2** has been investigated over the temperature range 10–300 K. Fitting of the magnetic susceptibility data for **2** by a simple Bleaney–Bowers expression yields a value for the singlet–triplet energy gap (J) of -139 cm^{-1}. The magnitude of the observed antiferromagnetic interaction is the smallest found in bipym-bridged copper(II) complexes for which the σ in-plane exchange pathway is operative. Extended-Hückel calculations have been used to analyse how the magnitude of the exchange coupling is influenced by small structural distortions in this family of complexes.

The co-ordination modes of squarate, $C_4O_4^{2-}$ (dianion of 3,4-dihydroxycyclobut-3-ene-1,2-dione) and its ability to transmit electronic effects between paramagnetic centres have attracted the attention of chemists during the last decade.[1–9] In the light of the structures of its metal complexes reported so far it is clear that chelation by this ligand is limited to some alkaline- and rare-earth metal cations.[1c,e,f,2b–d] The large value of the bite parameter of the squarate dianion accounts for this behaviour.[7d] As far as its co-ordination chemistry with 3d ions is concerned, a wide variety of modes has been found: monodentate,[3b,7d] μ-1,2-bis(monodentate),[3a,b,4a–c,5,7d,h,8d] μ-1,3-bis(monodentate)[6c,d,7b–g,8c] and tetrakis(monodentate).[3c,8b,9] Reported magnetic measurements of the structurally characterized squarato-bridged complexes revealed weak antiferromagnetic interactions, the largest one being -10.3 cm^{-1} for the singlet–triplet energy gap (J) in the complex $[Cu_2L_2(C_4O_4)(H_2O)]\cdot H_2O$,[7h] where L = *N*-[2-(diethylamino)ethyl]salicylideneaminate.

The magnetostructural features of the squarato-containing complexes deviate significantly from those of the related oxalato complexes where chelating and bis(chelating) co-ordination modes occur and strong antiferromagnetic interactions up to -385 cm^{-1} were achieved.[10] Coupled solution–solid state studies for squarate and oxalate complexes have shown that the analogy between the ligands (a set of four donor atoms, diprotic acids, planar stereochemistry and π-electron delocalization) is merely formal.[7f] The investigation of their co-ordinating properties toward divalent transition-metal ions is complicated by the formation of insoluble squarate- and oxalate-bridged polymers. The use of polydentate ligands alters the polymerization process and makes possible the isolation of species of lower nuclearity. Restricting ourselves to copper(II) for simplicity, the use of 2,2′-bipyridine (bipy) as outer ligand allowed the rational synthesis of the mononuclear $[Cu(bipy)(C_4O_4)(H_2O)]\cdot H_2O$ and its related dinuclear $[Cu_2(bipy)_2(C_4O_4)(H_2O)_2][NO_3]_2$ squarate-containing complexes,[7d] whereas the mononuclear $[Cu(bipy)(C_2O_4)(H_2O)]\cdot 2H_2O$, the chain $[Cu(bipy)(C_2O_4)]\cdot 2H_2O$ and the surprising di- and mono-nuclear $[Cu_2(bipy)_2(C_2O_4)(H_2O)_2]X_n\cdot[Cu(bipy)(C_2O_4)]$ [X = NO_3, ClO_4, BF_4 (n = 2) or SO_4^{2-} (n = 1)] compounds were prepared in the case of oxalate.[11–13]

When bipy is replaced by 2,2′-bipyrimidine (hereafter bipym), a ligand which can adopt both chelating and bis(chelating) co-ordination modes, the mononuclear mixed-ligand complex $[Cu(bipym)(C_2O_4)(H_2O)_2]\cdot 5H_2O$ and the sheet-like polymer $[Cu_2(bipym)(C_2O_4)]\cdot 5H_2O$ were prepared and structurally characterized.[14] Our first attempts concerning the related squarate derivatives provided us with the mixed-ligand species of formula $[Cu(bipym)(C_4O_4)(H_2O)_3]\cdot 2H_2O$ **1** and $[Cu_2(bipym)(C_4O_4)_2(H_2O)_6]$ **2**. In the present contribution we report on their preparation, structural determination and electronic characterization. The magnitude of the magnetic coupling in **2** is determined, compared to that in related bipym-bridged copper(II) complexes, and analysed in terms of observed structural distortions through theoretical calculations.

† *Supplementary data available:* see Instructions for Authors, *J. Chem. Soc., Dalton Trans.*, 1995, Issue 1, pp. xxv–xxx.

Non-SI unit employed: G = 10^{-4} T, eV ≈ 1.60×10^{-19} J.

Experimental

Materials.—Squaric acid was obtained from Aldrich and purified by recrystallization from water. A dilithium squarate solution was prepared by adding the required quantity of solid lithium hydroxide monohydrate to an aqueous solution of squaric acid. 2,2′-Bipyrimidine from Lancaster Synthesis was used as received. Elemental analyses (C, H, N) were conducted by the Microanalytical Service of the Universidad Autónoma de Madrid (Spain). The metal content was determined by atomic absorption spectrometry.

Preparations.—$[Cu(bipym)(C_4O_4)(H_2O)_3]\cdot 2H_2O$ **1**. This compound was obtained in quantitative yield as a greenish yellow crystalline powder by mixing concentrated aqueous solutions (30 cm^3) of dilithium squarate (0.9 mmol) and (2,2′-bipyrimidine)copper(II) nitrate (1 mmol). The solid was collected by vacuum filtration, washed with cold water, ethanol and diethyl ether and stored over calcium chloride. Needle-shaped crystals of **1** suitable for X-ray investigation were obtained by slow evaporation of warm brown aqueous solutions containing $Li_2[C_4O_4]$ (0.25 mmol) and $[Cu(bipym)][NO_3]_2$ (0.5 mmol) (Found: C, 34.10; H, 3.75; Cu, 14.90; N, 12.65. Calc. for $C_{12}H_{16}CuN_4O_9$: C, 34.00; H, 3.80; Cu, 15.00; N, 13.20%).

$[Cu_2(bipym)(C_4O_4)_2(H_2O)_6]$ **2**. A maroon polycrystalline powder and well formed plate-like brown crystals were formed by slow evaporation of aqueous solutions (230 cm^3) containing $Li_2[C_4O_4]$ (0.5 mmol) and $[Cu_2(bipym)][NO_3]_4$ (1 mmol). Crystals of **2**, also suitable for X-ray investigation, were obtained by slow diffusion in an H-tube {aqueous solutions of $Li_2[C_4O_4]$ and $[Cu_2(bipym)][NO_3]_4$ were introduced in each arm}. Analytical data on powdered samples (C, H, N) deviated significantly from those expected for **2** and revealed slight contamination by the chain compound $[Cu(C_4O_4)]\cdot 4H_2O$. The analytical data for the crystals were consistent with the formula of compound **2** (Found: C, 31.20; H, 2.75; Cu, 20.15; N, 8.85. Calc. for $C_{16}H_{18}Cu_2N_4O_{14}$: C, 31.15; H, 2.90; Cu, 20.60; N, 9.05%).

Physical Techniques.—Infrared spectra were recorded on a Perkin-Elmer 1750 FTIR spectrophotometer as KBr pellets in the 4000–300 cm^{-1} region, electronic spectra of dimethyl sulfoxide (dmso) and Nujol mull samples on a Perkin-Elmer Lambda 9 spectrophotometer, and variable-temperature ESR spectra with a Brüker ER 200D spectrometer equipped with a nitrogen cryostat. Magnetic susceptibility measurements of a 80 mg sample of complex **2**, composed of non-oriented crystallites, were made in the range 10–300 K with a fully automated AZTEC DSM5 pendulum-type susceptometer equipped with a TBT continuous-flow cryostat and a Brüker BE15 electromagnet, operating at 1.8 T. The compound $Hg[Co(NCS)_4]$ was used as a susceptibility standard. Diamagnetic corrections of the constituent atoms were calculated from Pascal constants and found to be -287×10^{-6} cm^3 mol^{-1}. The value 60×10^{-6} cm^3 mol^{-1} was used for the temperature-independent paramagnetism of the copper(II) ion.

Crystal Structure Determination and Refinement.—Diffraction data for complexes **1** and **2** were collected at 294 K with an Enraf-Nonius CAD-4 diffractometer using graphite-monochromated Mo-Kα radiation (λ = 0.710 73 Å). Crystal parameters and refinements results are listed in Table 1. The unit-cell parameters were derived from least-squares refinement of the setting angles of 25 reflections with 2θ angles in the ranges 32–45 and 28–45° for compounds **1** and **2**, respectively. Three reference reflections monitored throughout each data collection showed no significant decay. The usual corrections for Lorentz and polarization effects were carried out. In each case correction for absorption was done by the Gaussian integration method.[15]

The structures of complexes **1** and **2** were solved by direct methods and refined by full-matrix least-squares methods. All non-hydrogen atoms were refined anisotropically. Hydrogen atoms were located in Fourier-difference maps and refined isotropically. In the final refinement cycles an extinction parameter was adjusted (3.203×10^{-7} and 3.508×10^{-8} for **1** and **2**, respectively). The final full-matrix least-squares refinement on F, minimizing $\Sigma[w(|F_o| - |F_c|)^2]$, including 3158 (**1**) and 2226 (**2**) reflections with $I \geqslant 2\sigma(I)$, converged at R and R' indices of 0.031 and 0.033 for **1** and 0.028 and 0.037 for **2**. In the final difference map the residual maxima and minima were 0.33 and -0.12 e $Å^{-3}$ for **1** and 0.76 and -0.33 e $Å^{-3}$ for **2**. All calculations were carried out on a MICRO-VAX II computer with the Enraf-Nonius Structure Determination Programs.[16] The scattering curves, with anomalous scattering terms included, were those of Cromer and Waber.[17] The final atomic coordinates for non-hydrogen atoms and selected bond lengths and angles for compounds **1** and **2** are given in Tables 2–5.

Additional information available from the Cambridge Crystallographic Data Centre comprises H-atom coordinates, thermal parameters, and remaining bond lengths and angles.

Results and Discussion

Structures of Complexes **1** *and* **2**.—The structure of complex **1** consists of neutral mononuclear $[Cu(bipym)(C_4O_4)(H_2O)_3]$ units (Fig. 1) and water of hydration. The molecular units are linked by hydrogen bonds involving the three unco-ordinated squarate oxygens, all water molecules and the N(4) atom from bipym. The copper atom has a slightly distorted, elongated octahedral co-ordination with two bipym nitrogen atoms [2.019(2) and 2.036(2) Å for Cu–N(1) and Cu–N(2)], one squarate oxygen atom [1.953(1) Å for Cu–O(2)] and one water oxygen [1.961(1) Å for Cu–O(7)] in the equatorial plane, and two weakly bonded axial water molecules [2.442(2) and 2.372(2) Å for Cu–O(5) and Cu–O(6)]. The angle subtended by bipym at the metal atom is far from the ideal value of 90° [80.33(7)° for N(1)–Cu–N(2)] because of the geometrical constraints of a bipyrimidinyl ring system. The copper atom is displaced only 0.035(1) Å out of the least-squares plane defined by the equatorial ligand atoms, toward the axial O(6) oxygen atom. The dihedral angles between the equatorial plane and the planes defined by bipym and squarate ligands are 6.3 and 23.2°, respectively.

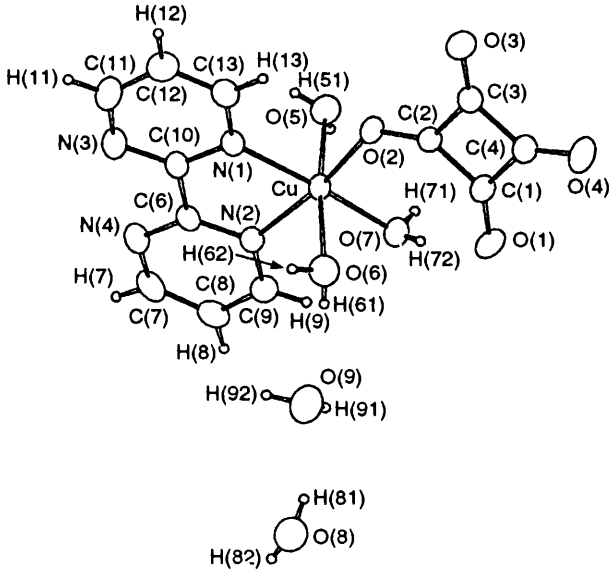

Fig. 1 Molecular structure of complex **1** showing the atom labelling: thermal ellipsoids are drawn at the 50% probability level

Table 1 Crystallographic data[a] for $[Cu(bipym)(C_4O_4)(H_2O)_3]\cdot 2H_2O$ **1** and $[Cu_2(bipym)(C_4O_4)_2(H_2O)_6]$ **2**

Compound	**1**	**2**
Formula	$C_{12}H_{16}CuN_4O_9$	$C_{16}H_{18}Cu_2N_4O_{14}$
M	423.82	617.42
Crystal system	Monoclinic	Triclinic
Space group	$P2_1/c$	$P\bar{1}$
a/Å	8.474(2)	6.310(2)
b/Å	11.501(1)	8.265(3)
c/Å	17.033(4)	10.367(5)
α/°		94.62(2)
β/°	91.73(1)	94.55(2)
γ/°		105.30(2)
U/Å^3	1659.3(9)	517.0(7)
Z	4	1
D_c/kg m^{-3}	1.696	1.983
$F(000)$	868	312
Crystal size/mm	0.46 × 0.12 × 0.11	0.40 × 0.17 × 0.05
μ(Mo-Kα)/mm^{-1}	1.372	2.146
Maximum, minimum transmission factors	0.878, 0.650	0.893, 0.603
Scan range/°	0.75 + 0.347 tan θ	0.80 + 0.347 tan θ
Octants of data collected	$hk \pm l$	$h \pm k \pm l$
No. unique reflections	3982	2486
No. reflections in the refinement,[b] N_o	3158	2226
No. parameters refined, N_p	300	200
R $\{ = [\Sigma(\|\|F_o\| - \|F_c\|\|)/\Sigma\|F_o\|]\}$	0.031	0.028
R' $\{ = [\Sigma w(\|\|F_o\| - \|F_c\|\|)^2/\Sigma w\|F_o\|^2]^{\frac{1}{2}}\}$[c]	0.033	0.037
S $\{ = [\Sigma w(\|\|F_o\| - \|F_c\|\|)^2/(N_o - N_p)]^{\frac{1}{2}}\}$	1.34	1.81

[a] Details in common: 2θ range 2–56°, scan type ω, scan speed 2.00° min^{-1}. [b] $I \geqslant 2\sigma(I)$. [c] $w = 4F_o^2/[\sigma_c^2 + (kF_o^2)^2]$, where σ_c is the standard deviation in F^2 based on counting statistics alone, and $k = 0.03$.

The structure of complex **2** is made up of centrosymmetric bipym-bridged, neutral, dinuclear $[Cu_2(bipym)(C_4O_4)_2(H_2O)_6]$ units (Fig. 2). The molecular units are linked by hydrogen bonds involving the water molecules and the unco-ordinated squarate oxygen atoms. Each copper atom has a slightly distorted elongated-octahedral co-ordination, with two bipym nitrogen atoms [2.088(2) and 2.052(2) Å for Cu–N(1) and Cu–N(3^I)], one squarato oxygen atom [1.922(1) Å for Cu–O(2)] and one water oxygen [1.999(2) Å for Cu–O(7)] in the equatorial plane, and two axial water molecules at longer distances [2.257(2) and 2.428(2) Å for Cu–O(5) and Cu–O(6)]. The angle subtended by bipym at the metal atom is 79.85(6)°, a value slightly smaller than that found in complex **1**. The metal atom is displaced by 0.096(1) Å from the least-squares planes defined by the equatorial ligand atoms, toward the axial O(5) oxygen atom. The same six-co-ordinate CuN_2O_4 chromophore is found in **1** and **2**. A comparison between the two similar co-ordination spheres reveals that the most noticeable differences are that the Cu–N (bipym) distances are significantly longer and the Cu–O (squarate) bond is shorter in the dinuclear complex, and that the Cu–O axial bond lengths differ by 0.17 Å in the dimer compared to 0.07 Å in the monomer. The dihedral angle between the equatorial plane of copper and the least-squares plane defined by the bridging bipym molecule is 11.4°, the metal atom deviating by 0.224(1) Å from the bipym plane. The plane of the squarato group makes an angle of 27.4° with the equatorial plane. The intramolecular metal–metal separation is 5.542(1) Å, a value which is among the largest observed for bipym-bridged copper(II) complexes.

The chelating bipym in the mononuclear complex is clearly distorted due to its co-ordination; it has a bite distance N(1)···N(2) of 2.616(2) Å, while the N(3)···N(4) distance is 2.765(3) Å. The asymmetry is also reflected in the bond distances and angles at C(6) and C(10) [1.338(3) and 1.326(3) Å for C(6)–N(2) and C(6)–N(4) and 115.0(2) and 119.0(2)° for N(2)–C(6)–C(10) and N(4)–C(6)–C(10); 1.339(3) and 1.324(3) Å for C(10)–N(1) and C(10)–N(3) and 114.8(2) and 118.6(2)° for N(1)–C(10)–C(6) and N(3)–C(10)–C(6)]. The bite distance of the bis(chelating) bipym in **2** is 2.657(2) Å. The carbon–carbon interring bond length in **1** [1.486(3) Å for C(6)–C(10)] is close to

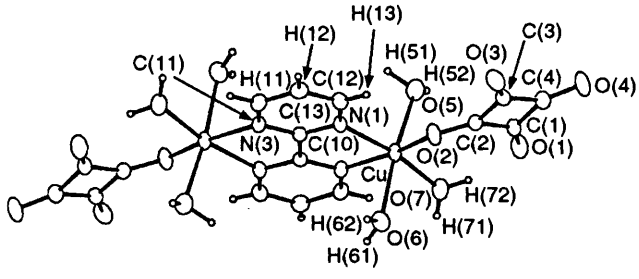

Fig. 2 Molecular structure of complex **2** along with the atom labelling; thermal ellipsoids are drawn at the 50% probability level

that found in free bipym in the solid state,[18] but significantly longer than that observed in **2** [1.467(3) Å for C(10)–C(10^I) (I $-x, -y, 1-z$)]. Furthermore, the bipym group is essentially planar in **2**, whereas it deviates somewhat from planarity in **1** [the dihedral angle between the two pyrimidine groups is 5.7(6)°].

The squarate dianion is almost planar in both complexes, the largest deviation from the mean plane being −0.011 Å at O(2) in **1** and −0.055 Å at O(4) in **2**. Its co-ordination to the metal atom as a unidentate ligand through the O(2) oxygen atom results in a longer C(2)–O(2) bond length [1.265(2) Å in **1** and 1.269(3) Å in **2**] as compared to the remaining C–O bonds [values ranging from 1.241(2) to 1.260(3) Å in **1** and from 1.240(2) to 1.260(2) Å in **2**] and causes significant deviations from the four-fold symmetry. In both compounds the effect of hydrogen bonding is also reflected in the squarate C–O bond lengths of the unco-ordinated oxygen atoms; the longer bonds of 1.260(3) Å [C(1)–O(1) in **1** and C(3)–O(3) in **2**] are each associated with two strong hydrogen bonds [2.741(2) for O(1)···O(6^{II}), 2.616(2) for O(1)···O(7) in **1**; 2.633(2) for O(3)···O(5^{IV}), 2.753(3) Å for O(3)···O(6^V) in **2** where II, IV and V refer to equivalent positions $1-x, \frac{1}{2}+y, \frac{3}{2}-z$; $x, 1+y, z$ and $1-x, 1-y, 1-z$, relative to the reference molecule at x, y, z]. The other unco-ordinated squarate oxygen atoms are involved in either only one strong or two weaker hydrogen bonds. The carbon–carbon bond lengths range from 1.445(3) to 1.475(3) Å

Table 2 Final atomic coordinates of non-hydrogen atoms for complex **1** with estimated standard deviations (e.s.d.s) in parentheses

Atom	*X/a*	*Y/b*	*Z/c*
Cu	0.326 87(3)	0.059 56(2)	0.862 79(1)
O(1)	0.531 9(2)	0.329 7(1)	0.803 40(9)
O(2)	0.539 6(2)	0.087 8(1)	0.905 88(9)
O(3)	0.887 0(2)	0.142 0(1)	0.965 85(9)
O(4)	0.887 1(2)	0.385 0(1)	0.867 3(1)
O(5)	0.205 9(2)	0.084 6(1)	0.989 98(9)
O(6)	0.431 7(2)	0.059 2(1)	0.735 24(9)
O(7)	0.273 7(2)	0.223 2(1)	0.843 41(9)
O(8)	0.175 0(2)	0.123 5(2)	0.448 3(1)
O(9)	0.181 6(2)	0.121 0(2)	0.616 5(1)
N(1)	0.347 6(2)	−0.112 4(2)	0.884 64(9)
N(2)	0.111 7(2)	0.004 6(2)	0.821 27(9)
N(3)	0.202 0(2)	−0.289 0(2)	0.877 0(1)
N(4)	−0.054 1(2)	−0.161 7(2)	0.820 8(1)
C(1)	0.630 6(2)	0.278 7(2)	0.848 3(1)
C(2)	0.631 7(2)	0.171 6(2)	0.892 7(1)
C(3)	0.792 1(2)	0.194 6(2)	0.921 8(1)
C(4)	0.791 8(2)	0.304 3(2)	0.876 9(1)
C(6)	0.083 0(2)	−0.108 3(2)	0.833 6(1)
C(7)	−0.171 0(3)	−0.095 3(2)	0.791 3(1)
C(8)	−0.151 5(3)	0.019 2(2)	0.772 8(1)
C(9)	−0.006 0(3)	0.067 9(2)	0.789 2(1)
C(10)	0.218 9(2)	−0.175 7(2)	0.866 8(1)
C(11)	0.327 9(3)	−0.342 8(2)	0.910 2(2)
C(12)	0.463 2(3)	−0.285 9(2)	0.932 4(1)
C(13)	0.470 8(2)	−0.168 3(2)	0.918 1(1)

Table 3 Final atomic coordinates for complex **2** with e.s.d.s in parentheses

Atom	*X/a*	*Y/b*	*Z/c*
Cu	0.154 71(4)	0.194 03(3)	0.303 77(2)
O(1)	0.232 5(3)	0.414 5(2)	0.008 7(2)
O(2)	0.310 1(3)	0.429 8(2)	0.324 5(1)
O(3)	0.441 8(3)	0.825 3(2)	0.352 1(2)
O(4)	0.340 9(3)	0.828 9(2)	0.041 1(2)
O(5)	−0.156 7(3)	0.250 1(2)	0.220 7(2)
O(6)	0.509 9(3)	0.155 2(2)	0.380 4(2)
O(7)	0.214 0(3)	0.133 7(2)	0.122 0(2)
N(1)	0.107 3(3)	0.221 7(2)	0.500 6(2)
N(3)	0.000 7(3)	0.051 1(2)	0.671 0(2)
C(1)	0.285 2(4)	0.528 9(3)	0.099 8(2)
C(2)	0.321 6(3)	0.535 1(2)	0.241 0(2)
C(3)	0.381 0(3)	0.715 3(3)	0.255 4(2)
C(4)	0.339 2(4)	0.716 8(3)	0.114 2(2)
C(10)	0.029 5(3)	0.075 5(2)	0.547 2(2)
C(11)	0.062 5(4)	0.189 3(3)	0.757 3(2)
C(12)	0.144 7(4)	0.347 4(3)	0.717 8(2)
C(13)	0.164 1(4)	0.360 3(3)	0.587 5(2)

in **1** and from 1.430(3) to 1.492(3) Å in **2**. As expected, the shortest C–C bond length is located between carbon atoms involved in the longer carbon–oxygen bonds. The C–C–C angles are close to 90° as usual [values ranging from 89.3(2) to 90.8(2)° in **1** and from 88.7(2) to 91.7(2)° in **2**] and the O–C–C angles vary between 130.7(2) and 138.4(2)° in **1** and between 131.3(2) and 137.0(2)° in **2**. These values are very close to those reported for other copper(II) complexes with monodentate squarate,[7d] but differ from those observed when squarate acts as a chelating or bis(chelating) ligand.[1c]

Intermolecular metal–metal separations shorter than 7 Å are: Cu···Cu^{III} (III $1-x, -y, 2-z$) 5.613(1) in **1** and Cu···Cu^{VI} (VI $1+x, y, z$) 6.310(2), Cu···Cu^{V} 6.585(2) and Cu···Cu^{VII} (VII $-x, -y, -z$) 7.727(2) Å in **2**.

We would like to finish this structural description with a brief structural comparison of complexes **1** and **2** with the analogous croconato complexes of formula $[Cu(bipym)(C_5O_5)(H_2O)_2]\cdot H_2O$ (mononuclear) and $[Cu_2(bipym)(C_5O_5)_2(H_2O)_2]\cdot 4H_2O$ (dinuclear) where $C_5O_5^{2-}$ is the dianion of croconic acid (4,5-dihydroxycyclopent-4-ene-1,2,3-trione).[19] The difference in metal co-ordination in the croconato pair is more pronounced than that in the squarato. So, whereas the copper atom has an elongated octahedral 4 + 2 co-ordination in the monomeric croconato complex, it exhibits a 4 + 1 + 1′ co-ordination in the dimeric one, with the second water molecule 2.95 Å away from copper. There is no equatorial water molecule in either compound, as the croconato group co-

Table 4 Selected interatomic distances (Å) and angles (°) for complex **1** with e.s.d.s in parentheses

Copper environment			
Cu–O(2)	1.953(1)	Cu–O(7)	1.961(1)
Cu–O(5)	2.442(2)	Cu–N(1)	2.019(2)
Cu–O(6)	2.372(2)	Cu–N(2)	2.036(2)
O(2)–Cu–O(5)	93.11(6)	O(5)–Cu–N(2)	87.10(6)
O(2)–Cu–O(6)	88.71(6)	O(6)–Cu–O(7)	86.44(6)
O(2)–Cu–O(7)	96.23(6)	O(6)–Cu–N(1)	97.72(6)
O(2)–Cu–N(1)	91.09(6)	O(6)–Cu–N(2)	92.16(6)
O(2)–Cu–N(2)	171.42(6)	O(7)–Cu–N(1)	171.67(6)
O(5)–Cu–O(6)	172.67(5)	O(7)–Cu–N(2)	92.34(6)
O(5)–Cu–O(7)	86.31(6)	N(1)–Cu–N(2)	80.33(7)
O(5)–Cu–N(1)	89.35(6)		
Squarate ligand			
O(1)–C(1)	1.260(3)	C(1)–C(2)	1.445(3)
O(2)–C(2)	1.265(2)	C(1)–C(4)	1.467(3)
O(3)–C(3)	1.241(2)	C(2)–C(3)	1.457(3)
O(4)–C(4)	1.244(3)	C(3)–C(4)	1.475(3)
Cu–O(2)–C(2)	128.9(1)	O(3)–C(3)–C(2)	134.3(2)
O(1)–C(1)–C(2)	135.0(2)	O(3)–C(3)–C(4)	136.2(2)
O(1)–C(1)–C(4)	134.6(2)	C(2)–C(3)–C(4)	89.5(2)
C(2)–C(1)–C(4)	90.4(2)	O(4)–C(4)–C(1)	135.1(2)
O(2)–C(2)–C(1)	138.4(2)	O(4)–C(4)–C(3)	135.6(2)
O(2)–C(2)–C(3)	130.7(2)	C(1)–C(4)–C(3)	89.3(2)
C(1)–C(2)–C(3)	90.8(2)		

Table 5 Selected interatomic distances (Å) and angles (°) for complex **2** with e.s.d.s in parentheses *

Copper environment			
Cu–O(2)	1.922(1)	Cu–O(7)	1.999(2)
Cu–O(5)	2.257(2)	Cu–N(1)	2.088(2)
Cu–O(6)	2.428(2)	Cu–N(3^{I})	2.052(2)
O(2)–Cu–O(5)	91.21(7)	O(5)–Cu–N(3^{I})	94.25(7)
O(2)–Cu–O(6)	84.41(7)	O(6)–Cu–O(7)	88.53(7)
O(2)–Cu–O(7)	99.42(7)	O(6)–Cu–N(1)	85.36(7)
O(2)–Cu–N(1)	87.02(6)	O(6)–Cu–N(3^{I})	90.84(6)
O(2)–Cu–N(3^{I})	166.36(6)	O(7)–Cu–N(1)	170.66(8)
O(5)–Cu–O(6)	174.23(6)	O(7)–Cu–N(3^{I})	93.21(7)
O(5)–Cu–O(7)	88.48(7)	N(1)–Cu–N(3^{I})	79.85(6)
O(5)–Cu–N(1)	98.19(7)		
Squarate ligand			
O(1)–C(1)	1.240(2)	C(1)–C(2)	1.458(3)
O(2)–C(2)	1.269(3)	C(1)–C(4)	1.492(3)
O(3)–C(3)	1.260(2)	C(2)–C(3)	1.430(3)
O(4)–C(4)	1.241(3)	C(3)–C(4)	1.468(3)
Cu–O(2)–C(2)	128.1(1)	O(3)–C(3)–C(2)	133.6(2)
O(1)–C(1)–C(2)	134.8(2)	O(3)–C(3)–C(4)	135.7(2)
O(1)–C(1)–C(4)	136.5(2)	C(2)–C(3)–C(4)	90.7(2)
C(2)–C(1)–C(4)	88.7(2)	O(4)–C(4)–C(1)	136.6(6)
O(2)–C(2)–C(1)	137.0(2)	O(4)–C(4)–C(3)	134.5(2)
O(2)–C(2)–C(3)	131.3(2)	C(1)–C(4)–C(3)	88.8(2)
C(1)–C(2)–C(3)	91.7(2)		

* Symmetry code: I $-x, -y, 1-z$.

ordinates in a bidentate fashion. The intramolecular metal–metal separation in **2** [5.542(1) Å] is appreciably longer than in the related croconato dimer [5.384(1) Å]. This structural feature is associated with longer Cu–N bonds and a smaller N–Cu–N angle in the former compound.

Infrared, Electronic and ESR Spectra of Complexes **1** *and* **2**.—The IR spectra of complexes **1** and **2** exhibit a weak band at 1790 cm^{-1} and a strong and broad absorption centred at 1490 cm^{-1} which are associated with stretching vibrations of non-coordinated C=O bonds[7a,20] and mixtures of C–C and C–O vibrations,[21] respectively. These spectral features together with the slight splitting observed in the latter one suggest that the symmetry for the squarate ligand is lower than D_{4h}, in line with the crystal structures observed. To high energy, the occurrence of a strong and broad absorption at 3440 cm^{-1} with a shoulder at 3250 cm^{-1} for **1** and a strong and broad peak at 3280 cm^{-1} for **2** are associated with the presence of the hydrogen bonds already discussed. The strong absorption of $C_4O_4^{2-}$ at 1490 cm^{-1} does not obscure the region for spectroscopic prediction of chelating and bis(chelating) bipym:[22] the presence of two sharp peaks of nearly equal intensity at 1585 and 1570 cm^{-1} (**1**) and of a single sharp peak at 1590 cm^{-1} (**2**) is consistent with the occurrence of chelating (**1**) and bis(chelating) (**2**) coordination modes of bipym. The 1250–1200 cm^{-1} region provides additional support for this prediction as reported previously for other bipym-containing copper(II) complexes:[19] two sharp weak peaks at 1220 and 1250 cm^{-1} for **1** and a sharp medium-intensity peak at 1235 cm^{-1} for **2**.

The visible region of the electronic spectra of mull samples of complexes **1** and **2** consists of two d–d bands at 700 and 1050 nm (**1**) and at 742 and 1200 nm (**2**) in agreement with the similarity observed for the metal surroundings in them. The shift toward lower wavelengths in **1** is in accord with the shorter equatorial distances in this compound. The main difference between the spectra in dmso solutions of **1** and **2** is the greater intensity of a peak centred at 455 nm (ε = 1600 dm^3 mol^{-1} cm^{-1}) in the latter which appears as a shoulder at 435 nm (ε = 500 dm^3 mol^{-1} cm^{-1}) in the former and is most likely associated with their different nuclearities. Very intense ligand-to-metal charge transfer and intraligand squarate and bipym transitions dominate at lower wavelengths.

The room-temperature polycrystalline X-band ESR spectrum of complex **1** looks like an axial doublet with $g_{\parallel}$ and $g_{\perp}$ values of 2.31 and 2.08, respectively. A very weak half-field forbidden transition is also observed. Such a pattern of g values is indicative of a $d_{x^2-y^2}$ orbital ground state in agreement with the distorted-octahedral environment of copper(II) in this complex. The spectrum remains practically unchanged on cooling to liquid-nitrogen temperature except for the $\Delta M_S = 2$ transition the intensity of which is significantly increased. This feature is most likely due to intermolecular interactions between the monomeric copper(II) units as previously reported for other structurally characterized mononuclear copper(II) complexes.[23] The ESR spectrum of **2** at room temperature consists of an asymmetric feature with $g_{\parallel}$ and $g_{\perp}$ values of 2.27 and 2.07, respectively. Its intensity quickly decreases upon cooling as expected for an excited triplet and a signal centred at 3129 G (g_{av} = 2.15) with a four-line hyperfine structure appears revealing the presence of monomeric impurities (see below).

Magnetic Properties of Complex **2**.—The thermal dependence of the molar magnetic susceptibility, χ_m, of complex **2** is shown in Fig. 3. The curve exhibits a behaviour which is characteristic of antiferromagnetically coupled copper(II) ions with a smooth maximum of the susceptibility at about 115 K. The increase of χ_m in the low-temperature region is due to the presence of a small amount of monomeric impurities as detected by ESR spectroscopy. Consequently, the experimental data were fitted by a modified Bleaney–Bowers expression for a dinuclear copper(II) complex [equation (1)] where J is the singlet–triplet

$$\chi_m = (2N\beta^2g^2/kT)[3 + \exp(-J/kT)]^{-1}(1 - \rho) + (N\beta^2g^2/2kT)\rho + 2N\alpha \quad (1)$$

$$\hat{H} = -J\hat{S}_1\cdot\hat{S}_2 \quad (2)$$

energy gap defined by the Hamiltonian (2); J expresses the intramolecular exchange interaction, $\hat{S}_1$ and $\hat{S}_2$ are quantum spin operators ($S_1 = S_2 = \frac{1}{2}$), N, g, β and T have their usual meaning and $N\alpha$ is the temperature-independent paramagnetism [60×10^{-6} cm^3 mol^{-1} per copper(II)] and ρ is the mass portion of uncoupled impurity, assumed to follow the Curie law and to have a molecular weight identical to that of the dimer. A least-squares fit of the data through equation (1) by a Simplex method leads to the values of -139 cm^{-1}, 2.17, 0.005 and 1.4×10^{-4} for J, g, ρ and R, respectively, where R is the agreement factor defined as $\Sigma[(\chi_m)^{obs} - (\chi_m)^{calc}]^2/\Sigma[(\chi_m)^{obs}]^2$.

The value of J for complex **2** suggests a relatively strong antiferromagnetic coupling between copper(II) ions separated by 5.542(1) Å. The overlap between the $d_{x^2-y^2}$ magnetic orbitals centred on each metal ion [the x and y axis being defined by the Cu–N(1) and Cu–N(3^I) bonds] accounts for this coupling, providing another example of the efficiency of the σ in-plane exchange pathway through bipym.[24] In this context, it deserves to be noted that a very weak admixture of the d_{z^2} orbital in the $d_{x^2-y^2}$ ground state is expected because the axial distances are longer than the equatorial ones. Magnetostructural data for bipym-bridged copper(II) complexes with a CuN_2O_4 chromophore and the σ in-plane exchange pathway operative are compiled in Table 6. An inspection of this table reveals that the antiferromagnetic interaction for **2** is the smallest in this family of complexes. In order to analyse qualitatively the influence of structural parameters on the value of the coupling, we have performed extended-Hückel calculations[27,28] on the dinuclear $(H_2O)_2Cu(bipym)Cu(H_2O)_2$ model system (Fig. 4) with a modified Wolfsberg–Helmholz formula.[29] The atomic parameters used are shown in Table 7.[28,30] These calculations

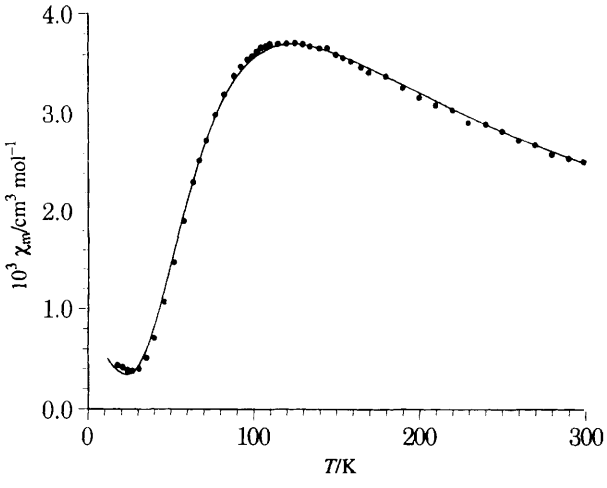

Fig. 3 Plot of the molar magnetic susceptibility of complex **2** as a function of temperature. The solid line represents the best fit to the data

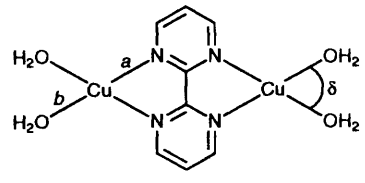

Fig. 4 Centrosymmetric model system used in the theoretical calculations. Average bond distances and angles for bipym are taken from the structures of the complexes in Table 6. Fixed values of 96° and 1.96 Å were kept for δ and *b*

Table 6 Selected magnetostructural data for bipym-bridged copper(II) complexes[a]

Compound	Cu–N/Å	Cu–O/Å	γ^b/°	$h_M{}^c$/Å	$d_{Cu\cdots Cu}{}^d$/Å	$-J$/cm^{-1}	Ref.
2	2.07	1.96	11.4	0.096	5.542(1)	139	This work
$[Cu_2(bipym)(H_2O)_4(SO_4)_2]\cdot 3H_2O$	2.04	1.97	5.1	0.075	5.456(1)	159	25
$[Cu_2(bipym)(C_5O_5)_2(H_2O)_2]\cdot 4H_2O$	2.02	1.97	14.4	0.187	5.384(1)	160	19
$[Cu_2(bipym)(NO_3)_4]$	2.01	1.96	3.5	0.021	5.371(1)	191	24, 26

[a] Average bond distances are given for each structure. [b] Dihedral angle between the mean equatorial plane around the metal ion and the bipym plane. [c] The height of the metal atom above the mean plane defined by the equatorial ligand atoms. [d] Metal–metal separation across bipym.

Table 7 Orbital exponents (contraction coefficients in double-ζ expansion given in parentheses) and energies used in the extended-Hückel calculations

Atom	Orbital	ζ_i (c_i)	H_{ii}/eV
Cu	4s	2.200	−11.40
	4p	2.200	−6.06
	3d	5.950 (0.5933), 2.300 (0.6168)	−14.00
C	2s	1.625	−21.40
	2p	1.625	−12.50
O	2s	2.275	−32.30
	2p	2.275	−14.80
H	1s	1.300	−13.60
N	2s	1.950	−26.00
	2p	1.950	−14.40

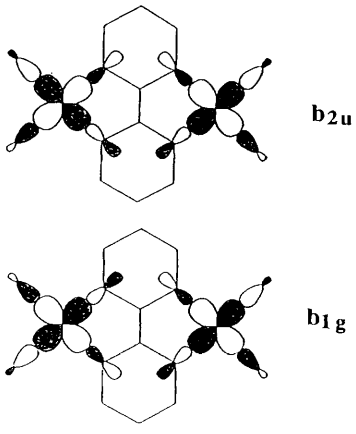

Scheme 1

afford the value of Δ which is the gap between the two singly occupied molecular orbitals in the dinuclear copper(II) unit (b_{1g} and b_{2u} in Scheme 1).

Taking into account that for a series of complexes with similar geometries and when the ferromagnetic terms are negligible $J \propto \Delta^2$,[31] it is clear that the larger Δ^2 is the greater the stabilization of the singlet. The variation of Δ^2 as a function of Cu–N, γ and h_M is depicted in Fig. 5. The influences of the Cu–O and Cu···Cu distances were not considered as the former remains practically unchanged along the series of compounds in question and the latter will depend on Cu–N and the planarity of the system. From Fig. 5 it is seen that increasing values of each of the parameters Cu–N, γ and h_M lead to decreasing values of Δ^2. It can also be inferred that small variations of Cu–N exert a greater influence on J than do distortions of the same order of magnitude of the other two factors. These results are qualitatively in good agreement with the experimental results quoted in Table 6. The nitrato derivative exhibits the smaller values for all the parameters, and consequently it has the stronger exchange coupling. A comparison between the sulfato and croconato derivative shows that the latter exhibits shorter values of Cu–N, but appreciably larger values of h_M and γ. The effects of the two groups of parameters cancel each other, and the resulting value

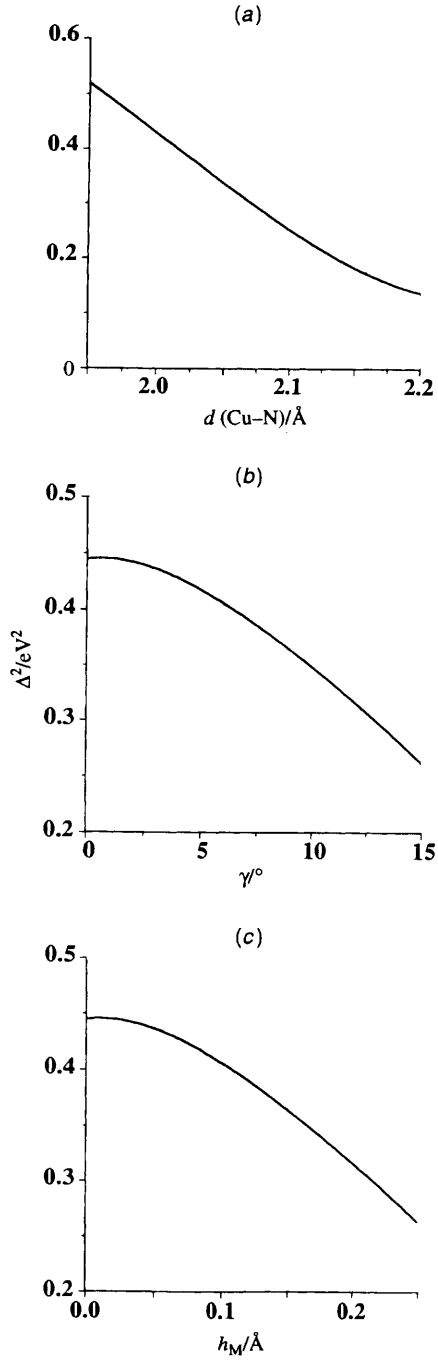

Fig. 5 Plots of the variation of Δ^2 as a function of (*a*) d_{Cu-N} (γ = 0 and h_M = 0), (*b*) γ (d_{Cu-N} = 2.0 and h_M = 0) and (*c*) h_M (d_{Cu-N} = 2.0 and γ = 0)

of the antiferromagnetic coupling is practically identical in the two species. Finally, although compound **2** has a smaller γ and

h_M than the croconato derivative, the appreciable increase of 0.05 Å in the Cu–N distance more than compensates for the effect of the former two parameters, resulting in the weakest exchange coupling in this series. In summary, these results show that the trend of the J values for these bipym-bridged complexes nicely reflects the structural distortions,[10] and that a rough estimate of the geometry dependence of J can be obtained by calculating the energy gap Δ at the simple Hückel level.

Acknowledgements

Thanks are due to the Dirección General de Investigación Científica y Técnica (DGICYT) (Spain) for partial financial support through Project PB91-0807-C02-01 and to the Servicio de Espectroscopía de la Universitat de València for instrumental facilities.

References

1 (*a*) J. C. Trombe, A. Gleizes and J. Galy, *C. R. Acad. Sci., Ser.* 2, 1986, **302**, 21; (*b*) J. F. Petit, J. C. Trombe, A. Gleizes and J. Galy, *C. R. Acad. Sci., Ser.* 2, 1987, **304**, 1117; (*c*) J. C. Trombe, J. F. Petit and A. Gleizes, *New J. Chem.*, 1988, **12**, 197; (*d*) J. F. Petit, A. Gleizes and J. C. Trombe, *Inorg. Chim. Acta*, 1990, **167**, 51; (*e*) J. C. Trombe, J. F. Petit and A. Gleizes, *Inorg. Chim. Acta*, 1990, **167**, 69; (*f*) J. C. Brouca-Cabarrecq, J. C. Trombe and A. Gleizes, *Eur. J. Solid State Inorg. Chem.*, 1991, **28**, 669; (*g*) A. Bouayad, C. Brouca-Cabarrecq, J. C. Trombe and A. Gleizes, *Inorg. Chim. Acta*, 1992, **195**, 193.

2 (*a*) C. Robl and A. Weiss, *Z. Naturforsch., Teil B*, 1986, **41**, 1485; (*b*) C. Robl and A. Weiss, *Z. Naturforsch., Teil B*, 1986, **41**, 1490; (*c*) C. Robl, V. Gnutzmann and A. Weiss, *Z. Anorg. Allg. Chem.*, 1987, **549**, 187; (*d*) C. Robl and A. Weiss, *Mater. Res. Bull.*, 1987, **22**, 373.

3 (*a*) Q. Chen, L. Ma, S. Liu and J. Zubieta, *J. Am. Chem. Soc.*, 1989, **111**, 5944; (*b*) Q. Chen, S. Liu and J. Zubieta, *Inorg. Chim. Acta*, 1989, **164**, 115; (*c*) Q. Chen, S. Liu and J. Zubieta, *Angew. Chem., Int. Ed. Engl.*, 1990, **29**, 70.

4 (*a*) O. Simonsen and H. Toftlund, *Inorg. Chem.*, 1981, **20**, 4044; (*b*) G. Bernardelli, P. Castan and R. Soules, *Inorg. Chim. Acta*, 1986, **120**, 205; (*c*) R. Soules, A. Mosset, J. P. Laurent, P. Castan, G. Bernardelli and M. Delamar, *Inorg. Chim. Acta*, 1989, **155**, 105; (*d*) P. Castan, D. Deguenon and P. L. Fabre, *Polyhedron*, 1992, **11**, 901.

5 J. P. Chesick and F. Doany, *Acta Crystallogr., Sect. B*, 1981, **37**, 1076.

6 (*a*) G. J. Long, *Inorg. Chem.*, 1978, **17**, 2702; (*b*) J. T. Wrobleski and D. B. Brown, *Inorg. Chem.*, 1979, **18**, 2738; (*c*) F. Lloret, M. Julve, J. Faus, X. Solans, Y. Journaux and I. Morgenstern-Badarau, *Inorg. Chem.*, 1990, **29**, 2232; (*d*) G. M. Frankenbach, M. A. Beno, A. M. Kini, J. M. Williams, U. Welp, J. E. Thompson and M. H. Whangbo, *Inorg. Chim. Acta*, 1992, **192**, 195.

7 (*a*) J. T. Reinpreeht, J. G. Miller, G. C. Vogel, M. S. Haddad and D. N. Hendrickson, *Inorg. Chem.*, 1980, **19**, 927; (*b*) C. Robl and A. Weiss, *Z. Naturforsch., Teil B*, 1986, **41**, 1341; (*c*) G. Bernardelli, D. Deguenon, R. Soules and P. Castan, *Can. J. Chem.*, 1989, **67**, 1158; (*d*) X. Solans, M. Aguiló, A. Gleizes, J. Faus, M. Julve and M. Verdaguer, *Inorg. Chem.*, 1990, **29**, 775; (*e*) I. Castro, J. Faus, M. Julve, M. Verdaguer, A. Monge and E. Gutiérrez-Puebla, *Inorg. Chim. Acta*, 1990, **170**, 251; (*f*) I. Castro, J. Faus, M. Julve, Y. Journaux and J. Sletten, *J. Chem. Soc., Dalton Trans.*, 1991, 2533; (*g*) M. Benetó, L. Soto, J. Garcia-Lozano, E. Escrivá, J. P. Legros and F. Dahan, *J. Chem. Soc., Dalton Trans.*, 1991, 1057; (*h*) C. E. Xanthopoulos, M. P. Sigalas, G. A. Katsoulos, C. A. Tsipis, C. C. Hadjikostas, A. Terzis and M. Mentzafos, *Inorg. Chem.*, 1993, **32**, 3743.

8 (*a*) D. M. Duggan, E. K. Barefield and D. N. Hendrickson, *Inorg. Chem.*, 1973, **12**, 985; (*b*) M. Habenschuss and B. C. Gerstein, *J. Chem. Phys.*, 1974, **61**, 852; (*c*) J. A. C. van Ooijen, J. Reedijk and A. L. Spek, *Inorg. Chem.*, 1979, **18**, 1184; (*d*) R. Soules, F. Dahan, J. P. Laurent and P. Castan, *J. Chem. Soc., Dalton Trans.*, 1988, 587; (*e*) A. Bencini, A. Bianchi, E. García-España, Y. Jeannin, M. Julve, V. Marcelino and M. Philoche-Levisalles, *Inorg. Chem.*, 1990, **29**, 963.

9 A. Weiss, E. Riegler and C. Robl, *Z. Naturforsch., Teil B*, 1986, **41**, 1329; 1333.

10 S. Alvarez, M. Julve and M. Verdaguer, *Inorg. Chem.*, 1990, **29**, 4500 and refs. therein.

11 W. Fitzgerald, J. Foley, D. McSweeney, N. Ray, D. Sheahan, S. Tyagi, B. Hathaway and P. O'Brien, *J. Chem. Soc., Dalton Trans.*, 1982, 1117.

12 I. Castro, J. Faus, M. Julve, M. C. Muñoz and W. Diaz, *Inorg. Chim. Acta*, 1991, **179**, 59.

13 M. Julve, J. Faus, M. Verdaguer and A. Gleizes, *J. Am. Chem. Soc.*, 1984, **106**, 3806; A. Gleizes, M. Julve, M. Verdaguer, J. A. Real, J. Faus and X. Solans, *J. Chem. Soc., Dalton Trans.*, 1992, 3209.

14 G. De Munno, M. Julve, F. Nicoló, F. Lloret, J. Faus, R. Ruiz and E. Sinn, *Angew. Chem., Int. Ed. Engl.*, 1993, **32**, 613.

15 P. Coppens, L. Leiserowitz and D. Rabinovich, *Acta Crystallogr.*, 1965, **18**, 1035.

16 B. A. Frenz, *The SDP-User's Guide* (*SDPVAX V.3*), Enraf-Nonius, Delft, 1983.

17 D. T. Cromer and J. T. Waber, *International Tables for X-Ray Crystallography*, Kynoch Press, Birmingham, 1974, vol. 4, p. 99, Table 2.2B.

18 L. Fernholt, C. Rømming and S. Sandal, *Acta Chem. Scand., Ser. A*, 1981, **35**, 707.

19 I. Castro, J. Sletten, L. K. Glærum, F. Lloret, J. Faus and M. Julve, *J. Chem. Soc., Dalton Trans.*, 1994, 2777.

20 C. G. Pierpont, L. C. Francesconi and D. N. Hendrickson, *Inorg. Chem.*, 1978, **17**, 3470; F. G. Baglin and C. B. Rose, *Spectrochim. Acta, Part A*, 1970, **26**, 2293.

21 M. Ito and B. West, *J. Am. Chem. Soc.*, 1963, **85**, 2580.

22 M. Julve, M. Verdaguer, G. De Munno, J. A. Real and G. Bruno, *Inorg. Chem.*, 1993, **32**, 795.

23 M. Julve, M. Verdaguer, J. Faus, M. Moratal, A. Monge and E. Gutiérrez-Puebla, *Inorg. Chem.*, 1987, **26**, 3520.

24 M. Julve, G. De Munno, G. Bruno and M. Verdaguer, *Inorg. Chem.*, 1988, **27**, 3160.

25 G. De Munno, M. Julve, F. Lloret, J. Cano and Andrea Caneschi, *Inorg. Chem.*, 1995, **34**, 2048.

26 G. De Munno and G. Bruno, *Acta Crystallogr., Sect. C*, 1984, **40**, 2030.

27 C. Mealli and D. M. Proserpio, Computer Aided Composition of Atomic Orbitals (CACAO Program), P. C. version, July 1992, kindly supplied by C. Mealli; see also *J. Chem. Educ.*, 1990, **67**, 3399.

28 R. J. Hoffmann, *J. Chem. Phys.*, 1963, **39**, 1397.

29 J. H. Ammeter, H. B. Bürgi, J. C. Thibeault and R. Hoffmann, *J. Am. Chem. Soc.*, 1978, **100**, 3686.

30 P. J. Hay, J. C. Thibeault and R. Hoffmann, *J. Am. Chem. Soc.*, 1975, **97**, 4884.

31 M. Verdaguer, O. Kahn, M. Julve and A. Gleizes, *Nouv. J. Chim.*, 1985, **9**, 325.

Received 6*th February* 1995; *Paper* 5/00670H